# ION INJECTION THROUGH FRINGE FIELDS OF DIPOLE MAGNETS[1]

B. Schillinger, T. Weiland, TH-Darmstadt, Germany
B. Langenbeck, GSI, Germany

*Abstract*

A new numerical procedure computing the ion optical transformation matrix up to second order will be presented. The magnetic flux distribution of an ESR dipole magnet is determined with the electromagnetic simulator MAFIA. The reference trajectory between the inflector magnet and the in–ring septum magnet, which enters the fringe field of the dipole in a tangential way, is integrated by using the calculated discrete field data. Along the trajectory, the radial derivatives of the field distribution are calculated and the linear ion optical matrix elements are determined by integrating the well known differential equations of the Hill type. We obtain the second order coefficients by integrating the corresponding driving functions as proposed by K. L. Brown and K. G. Steffen. The new procedure has been tested by applying it to a dipole with homogenous field and with parallel entrance and exit faces. The results are compared with calculations using the ion optical codes GIOS, RAYTRACE and TRANSPORT.

## 1 INTRODUCTION

Usual ion optical program packages describe beam lines as a sequence of elements like dipoles, quadrupoles, drift spaces etc., which are determined by some physical parameters. The treatment of fringe fields, however, is only possible in a restricted manner, e.g. approximated by three integrals [1].

Problems occur if the real fringe fields cannot be handled somehow idealized, as in case of the ion injection into the ESR [2], where the beam enters the first ESR dipole magnet tangentially. In addition the trajectory between the inflector magnet and the in–ring septum magnet cannot be described analytically. Thus a numerical treatment of the whole problem is the consequence, i.e. calculating the magnetic flux density using a static field solver, integrating the reference trajectory and computing the ion optical coefficients with respect of the numerical data.

In the following we restrict our calculations to deflecting magnets, with reference orbits lying in the symmetry plane of the optical device.

## 2 SECOND ORDER EXPANSION

We introduce a global coordinate system $\xi, \psi, \zeta$, with $\xi, \psi$ lying in the midplane of the deflecting magnet. The local coordinate system along the reference trajectory is $x, y, z$, where $x$ is the outer normal and $z$ the tangent to the trajectory in the midplane, as shown in figure 1. $\rho$ gives the radius of curvature at each point of the trajectory.

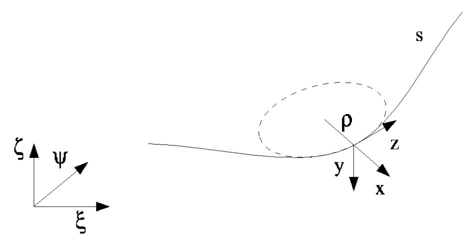


Figure 1: Global and local coordinate systems.

We want to describe the ion optical behaviour of a given deflecting magnet, i.e. we are interested in the map $x^1 = Ax^0$ of the initial vector $x^0 = (x_i^0)_{i=1,..,6}$ to the final vector $x^1 = (x_i^1)_{i=1,..,6}$ of the phase space coordinates $(x, x', y, y', l, \delta)$. Including second order effects, for each phase space component the map takes the expansion:

$$x_i^1 = \sum_{j=1}^{6}(x_i^1|x_j^0)x_j^0 + \sum_{j,k=1}^{6}(x_i^1|x_j^0x_k^0)x_j^0x_k^0 \qquad (1)$$

In order to get the first order coefficients $(x_i^1|x_j^0)$ the following differential equations for the so called principal trajectories $C$, $S$ and the Dispersion $D$ have to be solved:

$$C_x''(s) + k_x(s)C_x(s) = 0, \quad C_y''(s) + k_y(s)C_y(s) = 0,$$
$$S_x''(s) + k_x(s)S_x(s) = 0, \quad S_y''(s) + k_y(s)S_y(s) = 0, \qquad (2)$$

with boundary conditions $C(0) = 1$, $C'(0) = 0$, $S(0) = 0$, $S'(0) = 1$ and

$$D_x''(s) + k_x(s)D_x(s) = h(s), \qquad (3)$$

with boundary conditions $D(0) = D'(0) = 0$. The prime denotes derivation with respect to the path length $s$ along the reference trajectory. In the general case the curvature $h(s) = 1/\rho(s)$ and the factors $k_y(s) = -q/p_0 \partial B_y(s)/\partial x$ and $k_x(s) = h^2(s) - k_y(s)$ are non-constant and have to be determined, using the a priori given charge $q$ and momentum $p_0$ of the reference particle, the calculated magnetic flux density $B$ and its derivatives normal to the trajectory.

For the second order coefficients $q_{ijk} = (x_i^1|x_j^0x_k^0)$ also the second order field derivatives must be taken into account. The corresponding differential equations have the

[1] Work supported by GSI.

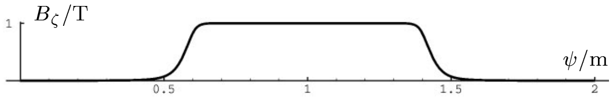


Figure 2: The field $B_\zeta(0, \psi, 0)$ of the test magnet.

form

$$q''_{ijk}(s) + k_x(s) q_{ijk}(s) = f_{ijk}(s), \quad (4)$$

with varying driving functions $f_{ijk}(s)$ and are listed in [3, 4]. These functions depend on the second field derivative normal to the reference trajectory. To get their optimum accuracy we consider to use for their determination field values on a larger box around the trajectory and to get the fields in its near neighbourhood by harmonic interpolation [5].

## 3 THE PROCEDURE

For arbitrary structures with midplane symmetry we propose the following procedure. First the magnetic field distribution is calculated using the static field solver S of the electromagnetic simulator MAFIA [6]. Then we determine the trajectory with the MAFIA tracking module TS3. Finally the differential equations (2), (3) and (4) are solved numerically using the computer algebra package MATHEMATICA[7].

## 4 A TEST MAGNET

To assure the accuracy of the solution, we tested the new procedure, implemented as part of the MAFIA TS3-module, on an idealized dipole magnet with parallel ends. The magnet length is $0.8$ m and the gap height is $0.08$ m Figure 2 shows $B_\zeta(0, \psi, 0)$, the magnetic flux density in the midplane over an interval of 2 m. The maximum is 1 Tesla and the field is constant in $\xi$ direction. In this case five transformation coefficients only depend on the injection and the ejection angle and therefore are given analytically [8].

Figure 3 shows $k_y(s)$ and $k_x(s)$, referring to the first normal derivative for an injection angle $\beta = 15°$ and a particle rigidity of 2 Tm calculated during the tracking process by using the discrete field data. They are functions of the arc length $s$.

In Figure 4 $r(s) = -q/(2p_0)\partial^2 B_y(s)/\partial x^2$ is plotted, which is used in the second order calculations.

Table 4 compares our first and second order results with the ion optical Codes GIOS [9] , TRANSPORT [10] and RAYTRACE [11].

## 5 THE ESR-DIPOLE

As mentioned in the introduction the ion optical treatment of the ion injection into the ESR is difficult, because the reference trajectory is not given analytically and lies about $2m$ in the fringe field region. Therefore the accurate simulation of the fringe fields has to be the first step. Figure 5 shows the simulation of the Rogowski profile at the dipoles exit face and figure 6 a radial cut to demonstrate the effects of the shims.

Figure 7 shows a cut of the simulated ESR-Dipole and the calculated trajectory. The particle rigidity is $8.5513$ Tm and the maximum field strength at the magnet midplane is $1.35$ T. We complete our studies with the plots of the calculated parameters (figure 8) and principal trajectories (figures 9).

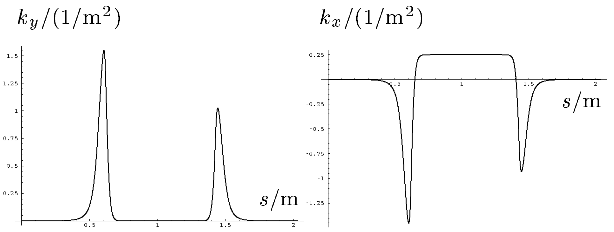


Figure 3: The left plot shows the stiffness parameter $k_y(s)$ which is proportional to the first order field derivative. $k_x(s)$ on the right side gives the quadratic path curvature $h(s)$ minus $k_y(s)$. Both parameters are functions of the arc length $s$.

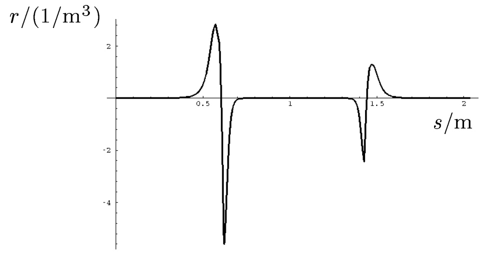


Figure 4: Weighted second order field derivative $r(s)$

## 6 CONCLUSION

The proposed procedure allows the determination of the first and second order ion optical coefficients in arbitrary field distributions with midplane symmetry. These coefficients will be used in TRANSPORT and MAD simulations of the ESR and its injection and ejection lines to define corrective measures (sextupole magnets).

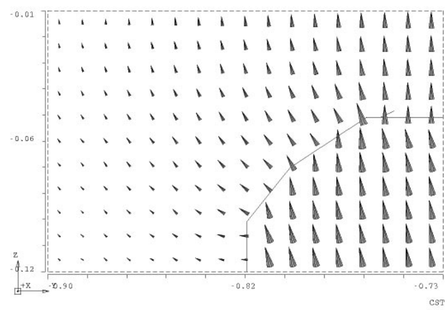


Figure 5: Fringe field at the exit face of the ESR-Dipole with the Rogowski profile.

| | GIOS | TRANSP. | RAYTR. | MAFIA |
|---|---|---|---|---|
| $(x^1\|x^0)$ | 1.01905 | 1.01905 | 1.01907 | 1.01905 |
| $(x^1\|x'^0)$ | 2.00866 | 2.0092 | 2.0084 | 2.00847 |
| $(x^1\|\delta^0)$ | 0.44333 | 0.44339 | 0.44320 | 0.44326 |
| $(x'^1\|x^0)$ | 0.00000 | 0.00000 | 0.00000 | -0.00011 |
| $(x'^1\|x'^0)$ | 0.98130 | 0.98130 | 0.98120 | 0.98112 |
| $(x'^1\|\delta^0)$ | 0.44209 | 0.44209 | 0.44201 | 0.44205 |
| $(y^1\|y^0)$ | 0.77318 | 0.77300 | 0.77304 | 0.77297 |
| $(y^1\|y'^0)$ | 1.86295 | 1.8620 | 1.8626 | 1.86250 |
| $(y'^1\|y^0)$ | -0.20084 | -0.20109 | -0.20000 | -0.20095 |
| $(y'^1\|y'^0)$ | 0.80943 | 0.80927 | 0.80954 | 0.80949 |
| $(l^1\|x^0)$ | 0.45051 | 0.45051 | 0.45044 | 0.45051 |
| $(l^1\|x'^0)$ | 0.45297 | 0.4531 | 0.4528 | 0.45291 |
| $(l^1\|\delta^0)$ | 0.02848 | 0.02794 | 0.02866 | 0.02848 |
| $(x^1\|x^0x^0)$ | 0.00000 | -0.00000 | 0.00000 | 0.00040 |
| $(x^1\|x^0x'^0)$ | 0.45219 | 0.4522 | 0.4521 | 0.45167 |
| $(x^1\|x^0\delta^0)$ | 0.08072 | 0.08071 | 0.08067 | 0.08063 |
| $(x^1\|x'^0x'^0)$ | 0.23105 | 0.2311 | 0.2308 | 0.23071 |
| $(x^1\|x'^0\delta^0)$ | 0.08553 | 0.08583 | 0.08740 | 0.087291 |
| $(x^1\|y^0y^0)$ | 0.06538 | 0.06787 | 0.06670 | 0.06503 |
| $(x^1\|y^0y'^0)$ | -0.30774 | -0.3111 | -0.3048 | -0.30764 |
| $(x^1\|y'^0y'^0)$ | -0.61383 | -0.6180 | -0.6115 | -0.61350 |
| $(x^1\|\delta^0\delta^0)$ | -0.44408 | -0.4441 | * | -0.44362 |
| $(y^1\|x^0y^0)$ | -0.03666 | -0.03606 | -0.03668 | -0.03631 |
| $(y^1\|x^0y'^0)$ | 0.35505 | 0.3523 | 0.3549 | 0.35854 |
| $(y^1\|x'^0y^0)$ | -0.54456 | -0.5546 | -0.2726 | -0.55062 |
| $(y^1\|x'^0y'^0)$ | 0.3310 | 0.3257 | 0.3309 | 0.33709 |
| $(y^1\|\delta^0y^0)$ | 0.31741 | 0.3446 | 0.3181 | 0.31960 |
| $(y^1\|\delta y'^0)$ | 0.36471 | 0.3875 | 0.3630 | 0.36596 |

Table 1: First and second order coefficients calculated with TRANSPORT, RAYTRACE and the new MAFIA procedure (in TRANSPORT notation).

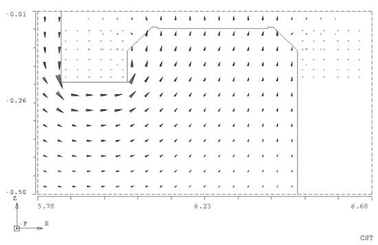

Figure 6: Radial cut which shows the lateral fringe fields, the position of the coils and the shims of the ESR-Dipole.

# 7 ACKNOWLEDGEMENT

We want to thank H. Wollnik, H. Weik and Winkler for doing the calculations of the test example with GIOS.

# 8 REFERENCES

[1] H. Wollnik, Optics of Charged Particles, Academic Press, Inc., 1987

[2] B. Franzke, et al., Commisioning of the Heavy Ion Storage Ring ESR, 2nd Europ. Part. Accel. Conf., Nice 1990

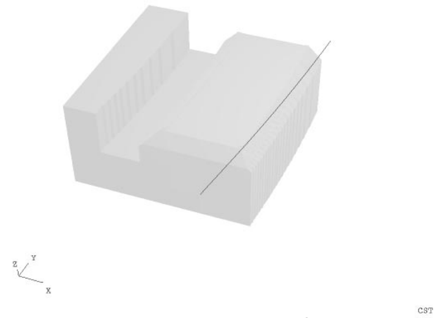

Figure 7: Simulated trajectory of the injection.

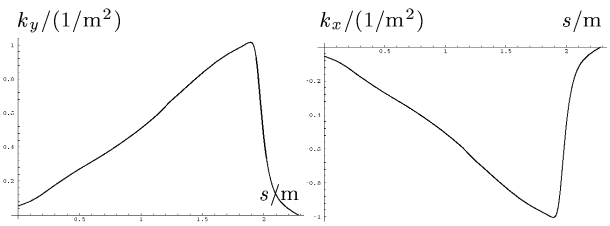


Figure 8: Stiffness parameters $k_y(s)$ and $k_x(s)$.

[3] K. L. Brown, A First and Second Order Matrix Theory for the Design of Beam Transport Systems, SLAC 75, 1967.

[4] K. G. Steffen, High Energy Beam Optics, Int. Publ., 1965.

[5] private communications H. Wollnik. See for example H. Wind, Evaluating a Magnetic Field Component from Boundary Observations only, Nucl. Inst. and Meth. 84 S.117-124, 1970

[6] The Mafia collaboration, User's Guide MAFIA Version 3.20, CST GmbH, Lauteschlägerstr.38, D–64289 Darmstadt

[7] S. Wolfram, Mathematica, Addison-Wesley Publishing Company, 1988

[8] B. Langenbeck, On the Ion Optics of Dipole Magnets with Parallel Ends Including Stray Field Effects, Nucl. Inst. Meth. Phy. Res. A258 S.515–524, 1987

[9] H. Wollnik at al., II. Phys. Inst., Uni Gießen, 1994.

[10] K. L. Brown at al., TRANSPORT, CERN 73–16, 1973

[11] S. Kowalski, H. A. Enge, Larboratory for Nuclear Science and Dep. of Phys., Cambridge, Massachusetts, USA, 1986.

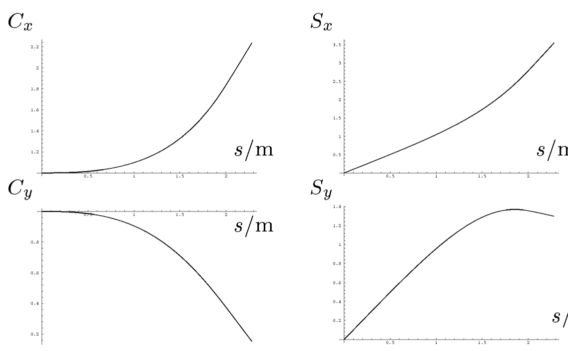


Figure 9: Principal trajectories $C_x(s)$, $S_x(s)$, $C_y(s)$ and $S_y(s)$.